Narrow linewidth 894 nm DFB lasers with laterally-coupled ridge-waveguide surface gratings fabricated using nanoimprint lithography

M. Dumitrescu, J. Telkkälä, J. Karinen, A. Laakso, J. Viheriälä,, T. Leinonen, J. Lyytikäinen, L. Toikkanen, M. Pessa

Optoelectronics Research Centre, Tampere University of Technology, Tampere, Finland

esa *Development of Extremely Narrow-Band Semiconductor Distributed Feedback Laser Technology*

Presentation outline

- Why DFB lasers with (LC-RWG) surface gratings?
- Particularities of LC-RWG surface gratings
- Application & target characteristics: ESA requirements
- Epilayer structures adjusted for LC-RWG gratings
- Coupling coefficient & modal selectivity
- Requirements on coupling coefficient
  and fabrication limitations
- End-mirror effects
- Device fabrication & fabricated device characteristics
- Towards improved device characteristcs
  - narrower spectral linewidth

The long path from idea to product: idea (new structure, new technology) + acquiring the facilities + proof of concept experiments + project proposal + detailed analysis + design + experiments + (many) iterations

Why DFB lasers with LC-RWG surface gratings?

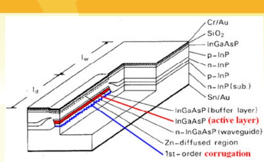

Akiba et al. *IEEE J. Quantum Electron.* **19**, 1052 (1983)

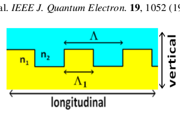

The conventional buried-grating fabrication techniques require overgrowth, which leads to problems with yield, performance and device cost.

Surface gratings:

✓single growth and processing sweep
=> better yield and lower cost
✓limited interaction between the carriers & the grating
=> more controllable performances
=> more stable (GaAs) devices
➢reduced coupling coefficient

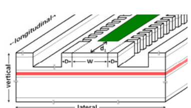

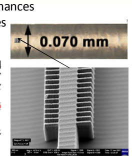

- Fabricated using UV-based nano-imprint lithography (UV-NIL), which enables pattern resolutions beyond the limitations set by the diffraction and scattering for the conventional techniques.
- basic dimensions: t, W, D,
- grating parameters: m, Λ, γ
- longitudinal parameters: L, R_1, R_2, d_1, d_2

Differences in coupling coefficient dependence on grating structure

DFB laser with a buried grating:

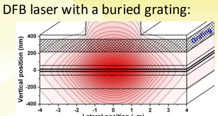

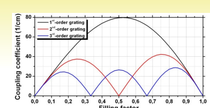

DFB laser with a LC-RWG grating:

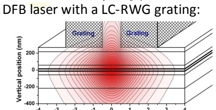

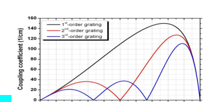

smaller Γ, higher Δn

=> high k is achievable

The effects of the grating order and filling factor on SMSR are not discussed in the literature (since buried-grating devices have been used).

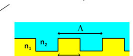

Λ_1/Λ = filling factor

$$\kappa = \frac{k_0}{2n_{eff}} \cdot (n_2^2 - n_1^2) \cdot \Gamma_g \cdot \frac{\sin(\pi m \gamma)}{\pi m}$$

=> with surface gratings high filling factor (i.e. small trench width) should be targeted

Both transverse and longitudinal mode discrimination have to be taken into account

Application & target characteristics

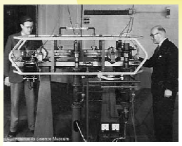

The 1955 Cesium Atomic Clock at the National Physical Laboratory, UK.: Cesium clocks measure frequency with an accuracy of from 2 to 3 parts in 10 to the 14th, with an averaging time of 5 days. i.e. 0.00000000000002 Hz; this corresponds to a time measurement accuracy of one second in 1,400,000 years. *It is the most accurate realization of a unit that mankind has yet achieved.*

In 1967, the 13th General Conference on Weights and Measures first defined the International System (SI) unit of time, the second, in terms of atomic time as *the duration of 9,192,631,770 cycles of microwave light absorbed or emitted by the hyperfine transition of cesium-133 atoms in their ground state undisturbed by external fields.*

The target: low-cost mass-produced atomic clock no larger than a sugar cube, which could run on an AA battery, yet accurate to one second in 300 years.

The competition: National Institute of Standards and Technology (NIST), Boulder, USA, under the Defense Advanced Research Projects Agency's (DARPA's) Chip-Scale Atomic Clock (CSAC) program

✓**Cesium atomic clocks** (*ESA project for developing narrow linewidth DFB lasers*)

- emission at 894.6 nm (tunable ± 2nm) (Cesium D1 line)
  => grating period $\Lambda \approx$ 140, 280, 420 nm
- output power ≥ 15 mW (@ I_{bias} < 100 mA)
- single mode CW operation with SMSR > 25 dB
- spectral linewidth **<< 1.5 MHz**

- ^{171,173}Yb
- ^{87,88}Sr
- ^{40}Ca+
- ^{27}Al+
- ^{199,201}Hg

- **Cooling lasers (1st, 2nd, ...)**
- **Auxiliary lasers**
- **Lattice lasers**
- **Probe lasers**

Epilayer structure

Active region (894 nm)

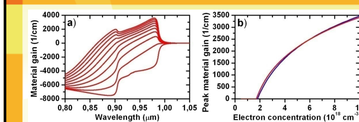

(a) Material gain simulated for 8 nm GaIn$_{0.20}$As/GaAs QW, and (b) the corresponding peak material gain compared with the variation reported in the literature (blue curve)

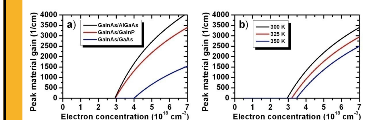

(a) The peak material gain simulated for 5 nm GaInAs/Al$_{0.30}$GaAs, GaInAs/GaIn$_{0.485}$P, and GaInAs/GaAs QWs, and (b) for 5 nm GaInAs/GaIn$_{0.485}$P QWs at 300, 325 and 350 K

For the emission at 894 nm GaInAs/GaAs QWs are too shallow and don't have high enough gain for effective operation.

GaInAs/AlGaAs or GaInAsP/GaAsP QWs would be deep enough, but the growth temperatures for GaInAs and AlGaAs are quite different and it is not recommended to use AlGaAs next to GaInAs QWs for reliability reasons .

The experimental studies indicate that the group V elements ratio in GaInAsP/GaAsP QWs is not easily controllable.

=> GaInAs/GaInP active regions (GaInP can be used as etch-stop)

Epilayer structure

Waveguide and cladding layers

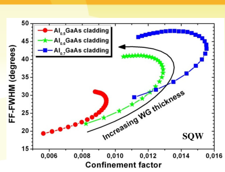

High QW confinement factor
- Small threshold current

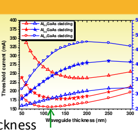

Higher Al-content in the cladding layer
- Wider far-field
- Narrower near-field → cladding thickness can be reduced (fabrication of the grating is easier), but coupling coefficient is smaller due to smaller achievable Γ_g

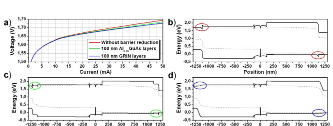

$$\kappa = \frac{k_0}{2n_{eff}} \cdot (n_2^2 - n_1^2) \cdot \Gamma_g \cdot \frac{\sin(\pi n \gamma)}{\pi n}$$

"Barrier reduction" layers added to GaAs-Al$_{0.7}$GaAs interfaces in order to improve current-voltage characteristics.

Epilayer structure

(for high grating coupling coefficient)

✓single GaInAs quantum well (QW)
✓120 nm GaInP waveguide (WG),etch-stop layer.
✓100 nm Al$_{0.3}$Ga$_{0.7}$As barrier-reduction layers
✓1000 nm thick Al$_{0.7}$Ga$_{0.3}$As cladding layers,
✓200 nm GaAs contact layer on the *p*-side.

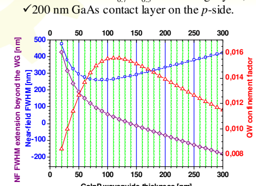

The QW confinement factor is usually maximized for low threshold and high bandwidth but this affects the coupling coefficient.

Surface gratings have low coupling coefficients (??)

Drastic changes of the epilayer structure in order to extend the optical field penetration into the cladding affect other critical parameters and small changes do not bring significant coupling coefficient improvement.

Etching depth should be used to ensure adequate coupling coefficient
- ⇒**Etching through the active region increases dramatically the losses**
- ⇒**Etching should be stopped above the active region (is this enough?)**

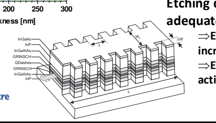

Coupling coefficient calculation

9

According to coupled-wave theory:

$$\kappa = \frac{k_0}{2n_{eff}} \cdot \frac{\int_{-\infty}^{\infty}\int_{-\infty}^{\infty} \Delta\varepsilon(x,y,z)\cdot\Psi^2(x,y)\,dxdy}{\int_{-\infty}^{\infty}\int_{-\infty}^{\infty}\Psi^2(x,y)\,dxdy}$$

Dielectric perturbation $\Delta\varepsilon_m(x,y,z)$ for m-th order rectangular-shaped grating:

$$\Delta\varepsilon_m(x,y,z) = \left[n_2(x,y)^2 - n_1(x,y)^2\right]\cdot\frac{\sin(\pi m\gamma)}{\pi m}$$

$$\kappa = \frac{k_0}{2n_{eff}}\cdot\frac{\sin(\pi m\gamma)}{\pi m}\cdot\left(\frac{\int_{-\infty}^{\infty}\int_{-\infty}^{\infty} n_2^2(x,y)\Psi^2(x,y)dxdy}{\int_{-\infty}^{\infty}\int_{-\infty}^{\infty}\Psi^2(x,y)dxdy} - \frac{\int_{-\infty}^{\infty}\int_{-\infty}^{\infty} n_1^2(x,y)\Psi^2(x,y)dxdy}{\int_{-\infty}^{\infty}\int_{-\infty}^{\infty}\Psi^2(x,y)dxdy}\right)$$

Conventional approximation

$$\approx k_0\cdot(n_2 - n_1)\cdot\Gamma_g\cdot\frac{\sin(\pi m\gamma)}{\pi m}$$

=> over-estimatimation

$$\kappa = \frac{k_0}{2n_{eff}}\cdot(n_2^2 - n_1^2)\cdot\Gamma_g\cdot\frac{\sin(\pi m\gamma)}{\pi m}$$

$$\kappa = \frac{k_0}{2n_{eff}}\cdot(n_{eff,2}{}^2 - n_{eff,1}{}^2)\cdot\frac{\sin(\pi m\gamma)}{\pi m}$$

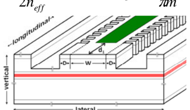

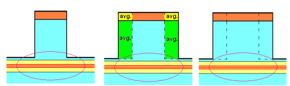

$$n_{eff,i} = \sqrt{\frac{\int\Psi^2(x,y)\cdot n_i^2(x,y)\cdot dx\cdot dy}{\int\Psi^2(x,y)\cdot dx}}$$

under-estimatimation possible

Coupling coefficient calculation
(effect of approximations)

10

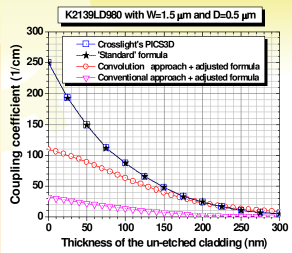

Third-order LC-RWG grating coupling coefficient values calculated with the standard formula (stars), with the adjusted formula and conventional method (triangles), with the adjusted formula and convolution method (circles) and obtained with PICS3D (squares)

The 'standard' formula for calculating the coupling coefficient is over-estimating the LC-RWG grating coupling coefficient

$$\kappa = \frac{\kappa_0}{2n_{eff}}\cdot\left(n_2^2 - n_1^2\right)\cdot\Gamma_g\cdot\frac{\sin(\pi m\gamma)}{\pi m} \approx k_0\cdot(n_2 - n_1)\cdot\Gamma_g\cdot\frac{\sin(\pi m\gamma)}{\pi m}$$

over-estimatimation since $2n_{eff} > (n_2 + n_1)$

The adjusted formula can produce under-estimation if the optical field is calculated separately for each grating section

$$\kappa = \frac{k_0}{2n_{eff}}\cdot(n_{eff,2}{}^2 - n_{eff,1}{}^2)\cdot\frac{\sin(\pi m\gamma)}{\pi m}$$

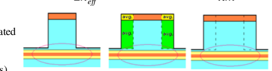

$(neff_{2\_conventional} - neff_{1\_conventional}) < (neff_{2\_convolution} - neff_{1\_convolution})$

(for certain dimensional ranges)

SMSR calculation

11

SMSR depends mostly on the bias current and the mirror loss margin, Δα:

$$SMSR(dB) \approx 10\log_{10}\left(\frac{\Delta\alpha + \Delta G}{\delta_G} + 1\right)$$

where $\delta_G = (\alpha_i + \alpha_m(\lambda_0))\beta_{sp}\eta_r\frac{1}{I/I_{th} - 1}$

$\Delta\alpha = \alpha_m(\lambda_1) - \alpha_m(\lambda_0)$ is the loss margin, $\Delta G = \Gamma g(\lambda_0) - \Gamma g(\lambda_1)$ is the modal gain margin and δ_G is the net modal gain for the main mode, β_{sp} is the spontaneous emission factor and η_r is the radiative recombination efficiency etc.

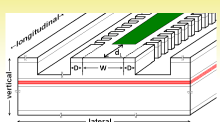

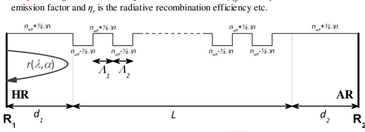

Modal positions and corresponding mirror losses are solved with Transfer Matrix Method

Threshold gain condition:

$$R_1\left|r(\lambda,\alpha)\right|^2 = 1$$

Phase condition:

r(λ,α) has to be real and positive

Both transverse and longitudinal mode discrimination have to be taken into account

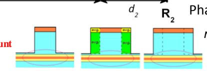

Transverse modal selectivity
(coupling coefficient discrimination)

12

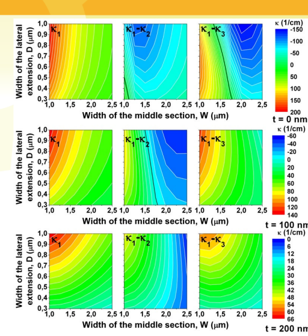

$$SMSR(dB) \approx 10\log_{10}\left(\frac{\Delta\alpha + \Delta G}{\delta_G} + 1\right)$$

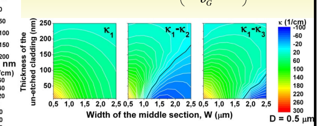

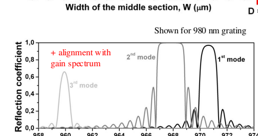

higher order transverse modes might have higher coupling coefficients but ...

Transverse modal selectivity
(confinement factor discrimination)

13

$$SMSR(dB) \approx 10\log_{10}\left(\frac{\Delta\alpha + \Delta G}{\delta_G} + 1\right)$$

- mirror loss discrimination
- **modal gain discrimination**

$$G_m = \frac{\iint \Psi_m^2(x,y) \cdot g_m(x,y)\, dxdy}{\iint_{\pm\infty} \Psi_m^2(x,y)\, dxdy}$$

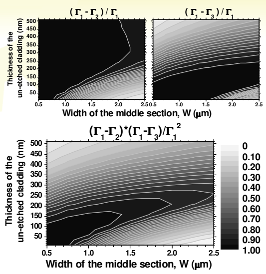

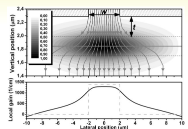

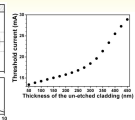

$$g_m(x,y)\big|_{act.reg\_under-ridge} = g$$

$$G_m \approx g\frac{\iint_{act\ reg,\ under\ ridge} \Psi_m^2(x,y)\, dxdy}{\iint_{\pm\infty} \Psi_m^2(x,y)\, dxdy} = g\Gamma_m$$

$$\Gamma_{1m} = \frac{g\Gamma_1 - g\Gamma_m}{g\Gamma_1} = \frac{\Gamma_1 - \Gamma_m}{\Gamma_1}$$

Longitudinal mode selectivity
(κL)

14

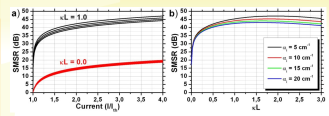

Simulated SMSR for a DFB structure with phase-matched facets, R_1 = 95 %, R_2 = 2 %, L = 500 µm and α_i = 5, 10, 15 or 20 cm^{-1} when (a) κ is either 0 or 20 cm^{-1} and I is varied, and (b) I/I_{th} = 3 and κ is varied

SMSR increases with κL only up to a certain κL value:

- small κL-value
  → not enough modal selectivity
- high κL-value
  → spatial hole burning
    → multiple longitudinal modes

=> κL≈1-2

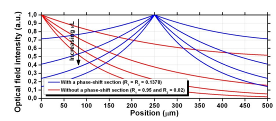

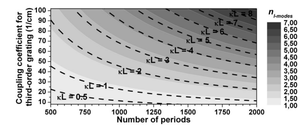

κL≈1-2 => 1-2 longitudinal modes within the grating stopband

Coupling coefficient
(targets & limits)

15

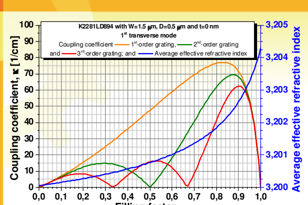

- The product κL=1-2 is important for longitudiunal mode selectivity
- High κ is critical only when devices have to be short (high modulation bandwidth)
- When the devices can be long (narrow linewidth) the technological limits matter more

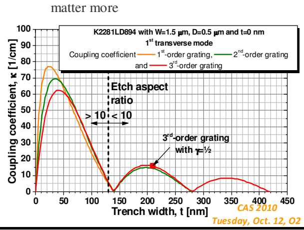

grating trench width is an essential parameter for achieving high κ

Modal degeneracy
(phase-shift section & mirror reflections)

16

Use of a phase-shift section

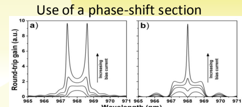

Devices without and with a phase-shift section when end facets have perfect anti-reflection (AR) coatings

the SMSR deteriorates rapidly for facet reflectivities of only a few percent due to the phase randomness of the facet reflections

HR

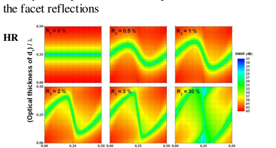

AR

Use of end-mirror reflections

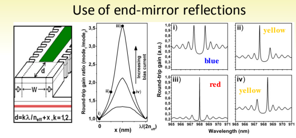

AR / high reflection (HR) –coated device without a phase-shift section when the distance between HR coating and the last grating period is varied

=> all DFB laser designs have an element of randomness as a result of the uncontrollable phase shift associated with the facet reflections.

End-mirror influence
(randomness in laser characteristics)

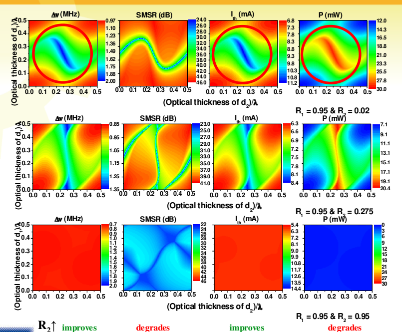

λ = 894 nm, n_{eff} = 3.2, k = 22 cm^{-1}, L = 700 µm, I_{bias} = 90mA, α_{eff} = 6 & α_i = 25 cm^{-1}

⇒ some important parameters are contradictory influenced by mirror phase (e.g. output power, bandwidth & linewidth)

Power – linewidth
(compromise evaluation)

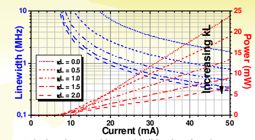

Calculated spectral linewidth (blue lines) and output power (red lines) variations for 1.2 mm long 894 nm LC-DFB structure with phase-matched R_1=0.95 & R_2= 0.02.

κ ≈ 22 cm^{-1}, L = 550 µm => κL=1.21
simulated Δν≈0.7 MHz, Pout≈20 mW

κ ≈ 22 cm^{-1}, L = 1000 µm => κL=2.2
simulated Δν≈0.35 MHz, Pout<10 mW

κ, L increase => Δν↓, Pout↓

achieving both P_{out}>15 mW and Δν < 1.5 MHz while 0.5 < κL < 2 (in order to have high SMSR) possible only in limited κ, L ranges

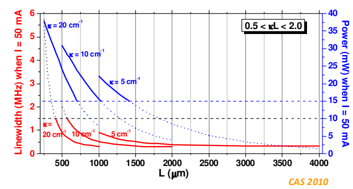

Nanoimprint lithography (NIL)

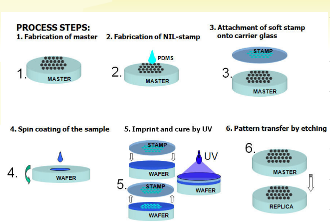

Contact technique involving pressure (small features => potential for very high pressure) and mechanical deformation => requirements:

- ✓ Stamp should be soft and flexible (to distribute pressure and to accomodate particle impurities and wafer non-flatness)
- ✓ Stamp should have minimal lateral deformation during imprinting (mostly for small features)
- ✓ Applied pressure should be low and uniform, despite varying imprinting area aspect ratio (avoid breaking the wafer and avoid local deformation of small size features – high local pressure)
- ✓ No temperature cycling and stress (=> UV-NIL => stamp should be UV transparent)
- ✓ Resist should have low viscosity – has to flow almost freely (surface tension forces)
- ✓ No bubbles should be present (vacuum process + low viscosity + surface tension)
- ✓ Small residual resist layer after imprint (residual layer has to be removed => smallest feature size is comparable with residual layer thickness)
- ✓ Durability of master template (contamination) and stamps

NIL stamp structure

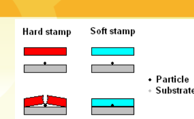

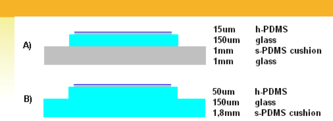

Three-layer NIL masks:

PDMS (polydimethylsiloxane), which is an UV transparent polymer

- Hard PDMS (h-PDMS) is used for copying the nanopatterns from the master (does not deform –good replication of small features where the local forces are very high - potential high deformation)
- Soft PDMS (s-PDMS), which is very poor for replicating small, sub 300 nm, patterns, is used as a cushion to ensure stamp softness.

Three-layer sequence:

- a thick s-PDMS cushion layer (softness, deformation, distribution of pressure),
- a thin layer of glass (which preserves the stamp flexibility but prevents the lateral stretching)
- a relatively thin nano-patterned h-PDMS layer.
- This three-layer soft stamp (B) may be placed on a relatively thick glass plate, generating a hard stamp (A).

accommodates particles and non-flat wafer

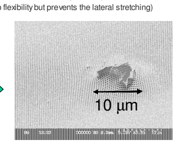

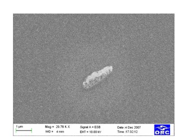

NIL imprinting

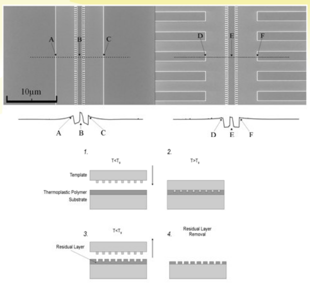

- Previous NIL masks produces thick residual layers (100 nm), which limits grating resolution
- New mask design with resist escape structures allow a reduction of residual layers below 10 nm → below 10 nm features are imprintable

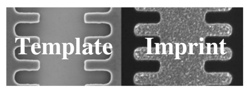

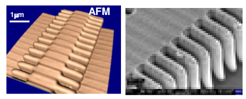

Improving the etching profile

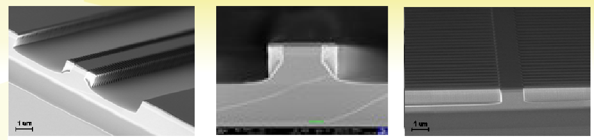

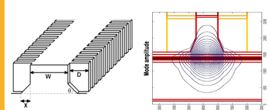

=> etching profile accuracy is essential in achieving high κ

lateral leakage control

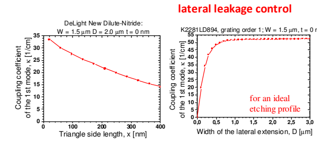

The coupling coefficient improvement with extended lateral gratings is derived mainly from improved etching profile and less from the increased lateral extension itself.

Higher κ by using wider lateral extension of the gratings & narrow trench widths

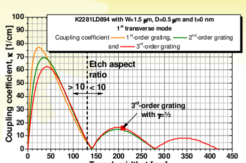

D=0.5 μm & ideal etching profile

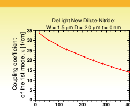

D=3.0 μm & ideal etching profile

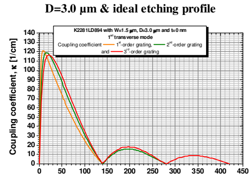

=> trench widths < 100 nm are desirable irrespective of grating order

Narrow trench etching experiments

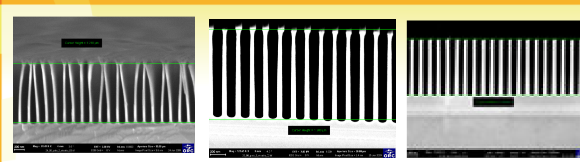

SEM views of gratings with period Λ=180 nm and trench widths of 140 nm (left panel),120 nm (middle panel) and 100 nm (right panel). Gratings were etched to a depth of 1.2, 1.2 and 1.1 μm in GaAs/AlGaAs

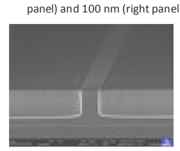

High aspect-ratio-patterns with BCB planarization:
-Better mechanical stability
-Less optical losses due scattering
-Higher bandwidth

=> 100 nm trench widths are achievable

Experimental evaluation of the coupling coefficient

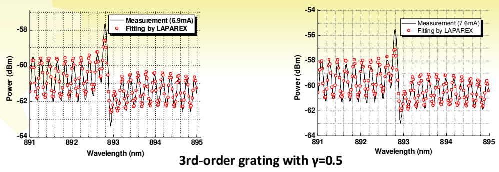

3rd-order grating with γ=0.5

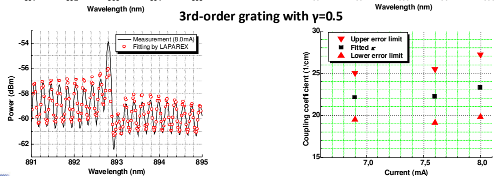

Coupling coefficient extraction by fitting simulated and experimental sub-threshold spectra

Fabricated 894 nm LC-DFB laser characteristics

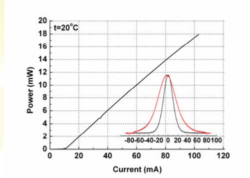

m = 3, γ = 0.5, κ = 22 cm⁻¹, L=550 µm, κL=1.21
(simulated / measured)

- emission at 894.6 nm (tunable ± 2nm)
- Ith ≈ 10 / 10 mA
- output power (@ I_{bias} = 90 < 100 mA) > 25 / ≈ 15 mW
- single mode CW operation with SMSR > 40 / 35 dB
- spectral linewidth (@ L=1000 µm) < 0.35 / ≈ 1.2 MHz

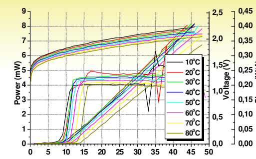

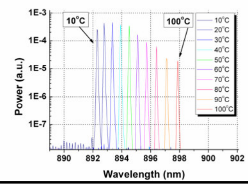

Linewidth evaluation @ 894 nm

spectral linewidth simulation (@ L=1000 µm) < 0.35 MHz

Technion

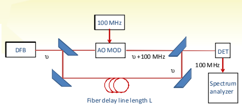

Self-homoheterodyne experimental set up

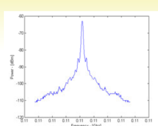

Self-homoheterodyne spectrum obtained with a 2 km long fiber (assuming Δν=1 MHz, the coherent length in fiber is ≈ 200 m)

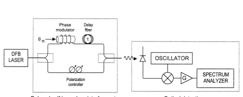

Short-delay self-homodyne experimental setup

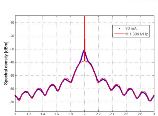

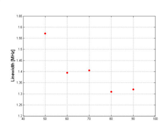

Short-delay homodyne spectrum fitting (left panel) linewidth evaluation at different bias levels (right panel) for a 1000 µm long LC-DFB laser

Further linewidth reduction

The spectral linewidth, *Δv*, of a laser due to spontaneous emission noise and carrier noise:

$$\Delta\nu = \frac{\Gamma R'_{sp}}{4\pi N_p}\left(1+\alpha_{eff}^2\right) = \frac{\Gamma R'_{sp} q \upsilon_g g_{th} V_{act}}{4\pi\eta_i (I-I_{th})}\left(1+\alpha_{eff}^2\right) = \frac{\Gamma q \upsilon_g^2 g_{th} n_{sp}}{4\pi\eta_i (I-I_{th})}(\alpha_i+\alpha_m)\left(1+\alpha_{eff}^2\right) = \frac{q\upsilon_g^2 n_{sp}}{4\pi\eta_i (I-I_{th})}(\alpha_i+\alpha_m)^2\left(1+\alpha_{eff}^2\right)$$

Decreasing α_m is more straightforward than decreasing α_i and α_{eff}. However, the output power is proportional to $\alpha_m/(\alpha_i+\alpha_m)$.

Linewidth and light-current measurements suggest that α_{eff} and α_i are higher than evaluated in simulations => significant linewidth reduction can be obtained by the reduction of α_i with epilayer and grating design and/or by the reduction of α_{eff} with a phase-shifted DFB design

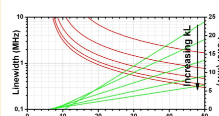

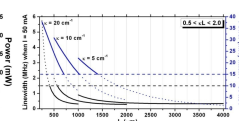

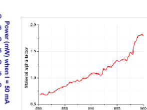

α_{eff}=6 was used in our linewidth simulations

Acknowledgements

esa *Development of Extremely Narrow-Band Semiconductor Distributed Feedback Laser Technology (Narrow DFB)*

Thank you!